

## ORBIT/ATTITUDE ESTIMATION WITH LANDSAT LANDMARK DATA

D. L. Hall and S. Waligora

Computer Sciences Corporation

### ABSTRACT

Several studies involving the use of Landsat Landmark data for orbit/attitude and camera bias estimation have been performed. The preliminary results of these investigations are presented. Three basic areas of work are covered. First, the Goddard Trajectory Determination System (GTDS) error analysis capability was used to perform error analysis studies. This provided preliminary guidelines for subsequent work with actual data. A number of questions were addressed including parameter observability and sensitivity, effects on the solve-for parameter errors of data span, density and distribution and a priori covariance weighting. The second area of investigation was the use of the GTDS differential correction (DC) capability with actual landmark data. The rms line and element observation residuals were studied as a function of the solve-for parameter set, a priori covariance weighting, force model, attitude model and data characteristics. Sample results are presented. Finally, verification and preliminary system evaluation of the Landsat NAVPAK system for sequential (extended Kalman Filter) estimation of orbit, attitude and camera bias parameters is given.

## SECTION 1 - INTRODUCTION

### 1.1 OVERVIEW

Landmark data obtained from Earth pictures taken by onboard spacecraft cameras can be used to: provide a means of autonomous navigation (References 1 and 2); aid in on-the-ground orbit and attitude determination (References 3 and 4), and aid in the geographical and geometrical registration of the Earth pictures for scientific users (Reference 4 and 5).

An important series of satellites that provides Earth pictures is the Landsat series. This paper describes two research (non-operational) software systems which have been developed to test the feasibility of orbit and attitude estimation using Landsat (Landsat-1 and -2) landmark data. The software development was performed by the authors and other staff members of the Computer Sciences Corporation (CSC) for the Goddard Space Flight Center (GSFC). Contained in this paper is an overview of the software systems (Section 2), summary of the mathematical models (Section 3), and some initial numerical results (Section 4). The remainder of this section reviews the Landsat picture data used by the two software systems, and summarizes the numerical results.

### 1.2 LANDSAT PICTURE DATA

The Landsat-1 and -2 spacecraft are Earth-stabilized with a low altitude (900 km), near polar (inclination 99 degrees), Sun-synchronous orbit. Their primary function is to take continuous pictures of the Earth. Hence, they are provided with an attitude control system that keeps them triaxially stable, i. e., the platform is (nominally) maintained in a horizontal position with respect to local vertical and faces forward (in the direction of the velocity). The spacecraft are equipped with a multispectral scanner (MSS), which enables them to take continuous scans 185 km wide, which are blocked to 185x185 km images on the ground. Scans over roughly 25 seconds yield the 185x185 images in

several spectral bands. The pictures are transmitted to the Earth as two-dimensional arrays of gray levels with picture coordinates consisting of line and element integers. Data from the return beam vidicon (RBV) camera system on Landsat-1 and -2, which also provides Earth pictures, is not used by the software systems discussed in this paper. Details of the Landsat configuration are given in Reference 6 and shown schematically in Figures 1-1 and 1-2. Figure 1-2 indicates the Landsat-1 and -2 ground coverage pattern. Picture data obtained by the MSS consist of intensity measurements in a two-dimensional grid. There are integer pairs (line and element) that specify a location within the grid. Each quantized location is called a pixel and has the dimensions (on the ground) of 79 meters in elevation (latitude) and 56 meters in azimuth (longitude). The identification that a picture coordinate pair is associated with the known geodetic coordinates of a point on Earth constitutes a single landmark observation. The creation of landmark observations is discussed in Section 2.1.3.

### 1.3 SUMMARY OF RESULTS

Initial numerical results of using Landsat-1 and -2 landmark data for S/C orbit/attitude estimation were obtained using two software systems. The Landsat NAVPAK system allows sequential orbit/attitude estimation using an extended Kalman filter (EKF). The Research and Development Goddard Trajectory Determination System (R&D GTDS) was modified to allow batch differential correction (DC) orbit/attitude estimation using Landsat data. The data set used to obtain preliminary numerical results is discussed in Section 4 and consists of 106 landmark observations over a five-minute Landsat pass.

Several numerical experiments were performed using both the EKF and DC. Effects studied included the choice of solve-for parameters, the influence of the a priori covariance matrix, the use of wheel rate data to aid attitude modeling and force model effects. The basic results are summarized below.

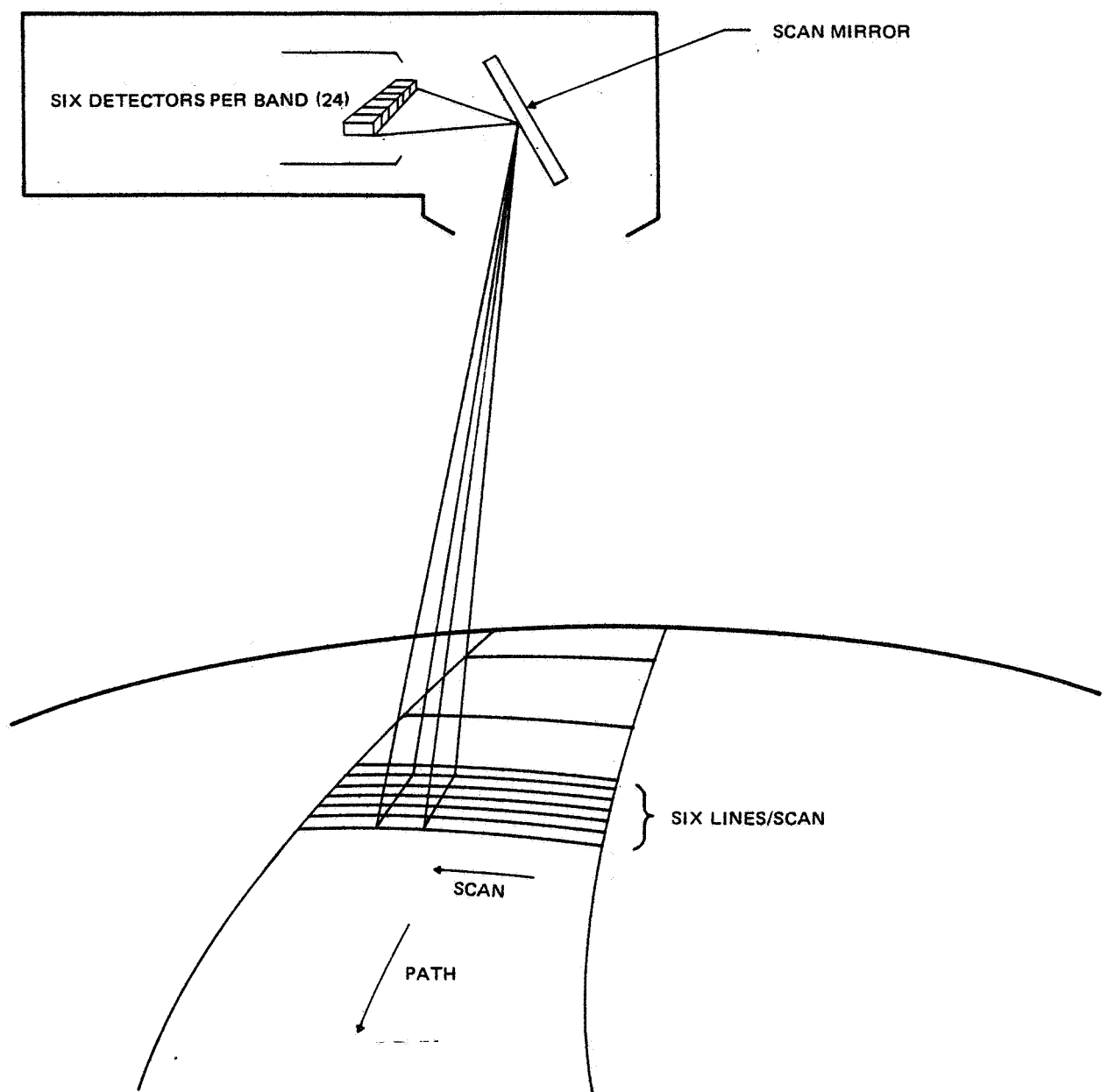


Figure 1-1. Landsat 1 and 2 Multispectral Scanner Coverage

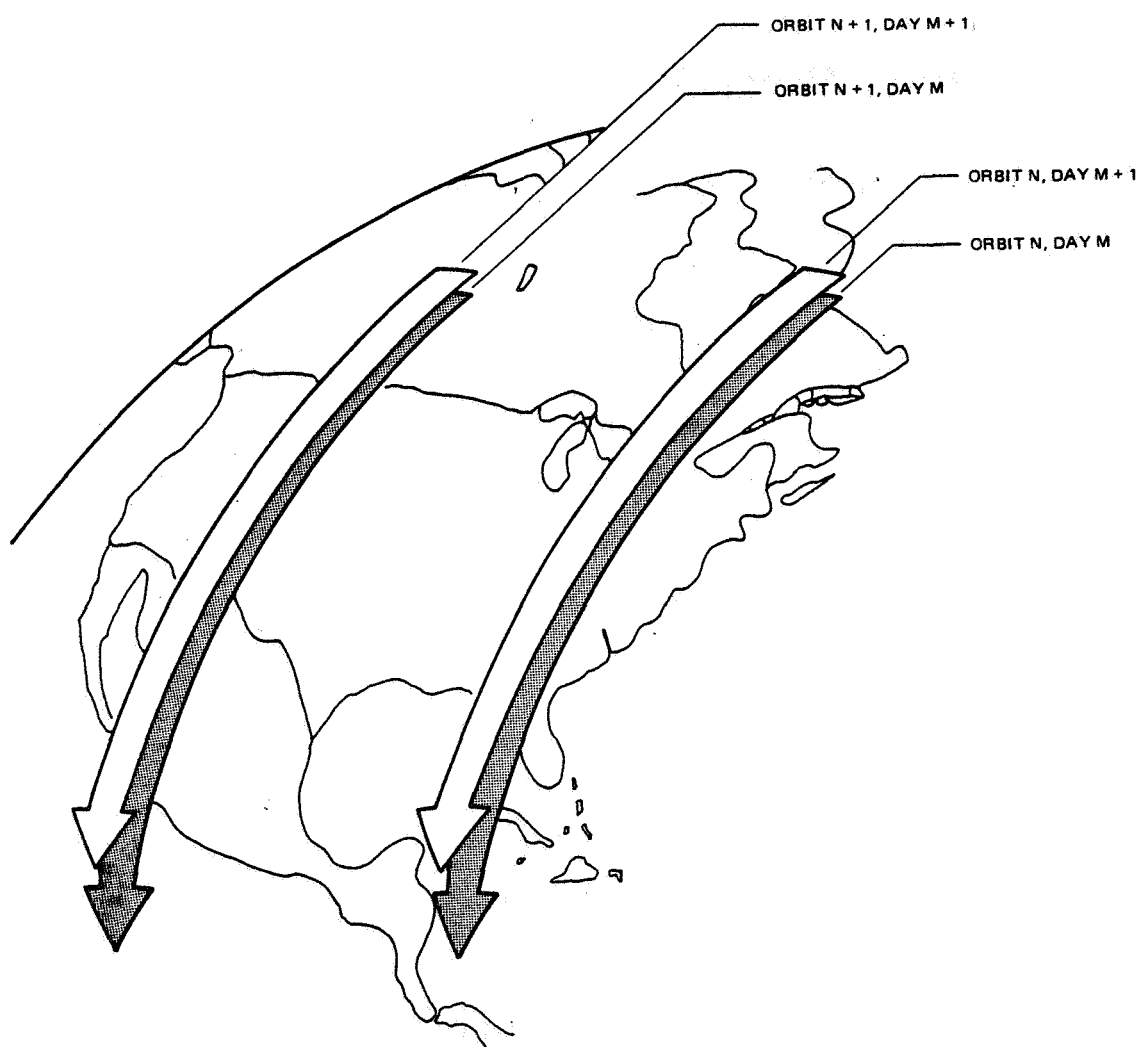


Figure 1-2. Landsat 1 and 2 MMS Ground Coverage Pattern

### Batch (DC) Orbit/Attitude Estimation Results

In the following results, the residuals are computed based on a converged differential correction solution. Parameters which are not estimated are set to a priori values annotated on the Landsat image associated with the start of the data set.

- The S/C orbital parameters and several coefficients of an attitude time series model can be estimated using batch processing of Landsat landmark data. For a five-minute data span rms residuals of 7.3 pixels and 9.2 pixels can be obtained for scan angle and elevation angles, respectively.
- The use of wheel rate data for attitude modeling significantly improves the fit, resulting in residuals of 2.7 and 3.6 pixels for scan and elevation angle when solving for S/C state and three attitude coefficients as above.
- The choice of a priori covariance matrix (particularly the ratio of the S/C state covariance to the attitude covariance) influences the final observation residuals by a factor of about 40% when varied over several orders of magnitude range.
- Camera biases are indistinguishable from constant attitude coefficients when solved for using a five-minute data span.
- The force model consisting of the two body gravitational attraction of the Earth,  $J_2$  nonspherical gravitational effect and drag model is completely adequate over a five-minute data span. More complicated models including higher order nonspherical geopotential terms, lunar/solar third-body effects, and solar radiation pressure affect the rms residuals by less than 0.01 pixel.

### Sequential (EKF) Orbit/Attitude Estimation Results

In the following results, the residuals are obtained after one pass of the EKF through the data set. The final values of the solve-for parameters are propagated back through the observation set to compute observation residuals.

- The NAVPAK EKF was able to estimate S/C orbit and constant attitude parameters using landmark data. For a five-minute data span, rms residuals of 14.7 pixels and 11.9 pixels can be obtained for scan angle and elevation angles, respectively.
- Wheel rate data provided a slight decrease of residuals for a continuous (without gaps) data set. A significant improvement was obtained with wheel rate data when the landmark data contained at least one gap. Hence the wheel rate data had a stabilizing effect.
- Variation of the a priori covariance matrix (the relative weighting between S/C orbit and attitude covariances) caused a variation of about 20% in the overall observation residuals.
- The EKF was unable to realistically estimate multiple coefficients for each component of attitude (roll, pitch and yaw).
- The camera biases were indistinguishable from constant attitude coefficients.

## SECTION 2 - SOFTWARE SYSTEM OVERVIEW

There are two research software systems described in this paper. The first is the Landsat NAVPAK (Navigation Package) system which provides for data preprocessing, Landsat image display and manipulation, observation creation, and orbit/attitude estimation using Landsat data via an extended Kalman filter. The second system is a portion of the Research and Development Goddard Trajectory Determination System (R&D GTDS) which has the capability to perform orbit/attitude estimation using Landsat data via a batch least squares or differential correction (DC) approach. The basic features of these systems are described in this section.

### 2.1 LANDSAT NAVPAK

The Landsat NAVPAK is a menu driven, interactive software (FORTRAN) system which has been implemented on a PDP 11/70 computer operating under the RSX-11D system. Reference 7 gives details of the mathematics, software and user instructions for NAVPAK. There are four basic functions performed by NAVPAK including data preprocessing, Landsat image display and manipulation, observation creation, and orbit/attitude estimation via an extended Kalman filter. Each of these functions is described below.

### 2.1.1 Data Preprocessing

The input data to the NAVPAK System are Landsat imagery received from Computer Compatible Tapes (CCTs), momentum wheel rate data from pre-processed data tapes, and user-specified estimation parameters. Another possible input is a R&D GTDS simulated observations tape, which can be used to verify the operation of the estimator. The data preprocessing function of NAVPAK provides for a manipulation of the input data to make it usable for the NAVPAK estimation and observation creation functions. The data preprocessing consists of the following.

Firstly, one or more single band Full Scene Images (FSIs) is reconstructed from a set of CCTs. Four CCTs are required to produce one image for each spectral band. This process is performed for each usable scene in a pass of Landsat imagery.

Secondly, on the IBM S/360-95 a raw wheel rate tape is converted to a PDP-11/70 compatible tape and the low frequency components of attitude (yaw, roll, and pitch) are determined. The tape is then moved to the PDP-11/70, where a file containing spacecraft body rates is created by removing the low frequencies, as described in Section 3.2.

For observation creation described in Section 2.1.3, Landmark reference chips and Super Search Areas are required. A reference chip is a 16 x 16 pixel area in a Landsat picture, which is centered on a landmark of known geodetic coordinates. Hence, the operator displays a Landsat picture (Section 2.1.2) and manually locates a position whose geodetic coordinates are known from, say, a reference map. The reference point is usually an easily recognizable feature, such as a road intersection, which has been accurately surveyed. The data preprocessor allows the user to extract a chip and store it on a file along with an identifying name and number and associated geodetic coordinates. The creation of a chip library is a one time only NAVPAK function.

Once a chip library exists, it is necessary to create a set of Super Search Areas (SSAs) to process a current pass of data. These SSAs are 100 x 100 pixel areas which are expected to contain areas which correspond to reference chips. Thus, for observation creation, each observation to be generated requires a SSA from the current pass of Landsat imagery and an associated reference chip (obtained from an original pass of Landsat data).

#### 2.1.2 Image Display and Manipulation

The second NAVPAK function is Landsat image display and manipulation on an International Imaging System (I<sup>2</sup>S) video device. A full 185km Landsat picture can be displayed on the I<sup>2</sup>S by a reduced mode in which every sixth line and every eighth element are displayed. Also, portions of a picture can be displayed at full resolution (viz. every pixel displayed). In addition, any portion of a picture may be displayed at an expanded (zoomed) scale with a zoom ratio up to 64 to 1. The zoom is obtained by a two-dimensional cubic interpolation scheme.

The video device has a cursor (electronic cross-hair marker on the screen) which can be moved manually by a track-ball. The image display and manipulation function of NAVPAK provides for a read out of the picture coordinates (line and element numbers) corresponding to the location of the cursor. A standalone program is available to use these picture coordinates, along with an estimate of the spacecraft orbit and attitude to compute the geodetic coordinates associated with the cursor location. Finally, NAVPAK allows a user to automatically drive the cursor to the picture coordinates which correspond to a specified geodetic coordinate pair  $(\phi, \lambda)$ . This latter is done using the geodetic annotation on the Landsat picture instead of estimated orbit/attitude parameters.

### 2.1.3 Observation Creation

The third function performed by Landsat NAVPAK is observation creation. For a current pass of Landsat imagery, there exists a set of chips (in the chip library) which correspond to geodetic locations within the pass. The data pre-processor has been used to create SSAs corresponding to those chips. Each observation is created by correlating a SSA with its associated reference chip. This is done by an automatic direct correlation algorithm. This results in the association of picture and time (from a picture in the current pass) and the geodetic coordinates of the landmark. These observations are then stored in an observations file to be used by the estimator.

### 2.1.4 Orbit/Attitude Estimation

The fourth function performed by Landsat NAVPAK is spacecraft orbit/attitude estimation using an extended Kalman filter. This filter has the capability of solving for 24 parameters including 6 state parameters (geocentric inertial Cartesian position and velocity components), 15 attitude coefficients, and 3 spacecraft camera biases. Attitude modeling is obtained by solving for coefficients of fourth-degree time polynomials for the roll, pitch and yaw angles. In addition, an option exists to use integrated high frequency momentum wheel rate data to model the high frequency attitude motion. The force model for the spacecraft motion includes atmospheric drag using a modified Harris-Priester model, the two-body gravitational attraction of the Earth and the  $J_2$  harmonic coefficient. Integration of the equations of motion are provided by a fourth-order Runge-Kutta method with modified Fehlberg coefficients. The transition matrix propagation is done by a Taylor series. Process noise is currently being implemented. The numerical results obtained in this study indicate that the force model is adequate for data spans not exceeding 10 minutes in length (i.e., a single pass over the United States).

A number of options exist for the operation of the filter and input and output. The data may be processed one point at a time with operator intervention at each point or an entire set of data processed. In addition, a data set may be processed iteratively such that the estimated parameters and covariance matrix for one iteration are propagated back to the first observation time to be used as a priori values for the succeeding iteration. Input data base management allows for control of the a priori solve-for parameters and covariance matrix, selection of force model terms, selection of solve-for parameters, control flags for fading memory, observation editing, process noise and use of wheel-rate data for attitude modeling. Output reports include initial conditions report, observation residuals output, end of iteration solve-for parameter and covariance matrix output. In addition the filter update history may be output. Details of the orbit/attitude mathematics are given in the next section.

## 2.2 R&D GTDS

The R&D GTDS is a very large (500k core) collection of FORTRAN subroutines to provide orbit/attitude determination, data simulation and error analysis for GSFC research. A number of data types are provided for, with state-of-the-art sophistication in spacecraft dynamic modeling and numerical techniques for orbit propagation. The fundamental mathematical specifications for this system are given by Reference 8. The system was enhanced to process Landsat landmark data (Reference 4). Specifically, orbit/attitude estimation can be done using Landsat landmark data by a batch weighted least-square method. The R&D GTDS does not have any capability for Landsat picture display and manipulation or observation creation (other than data simulation). For that reason, Landsat NAVPAK was used in this study to generate Landsat landmark observation data. Then, the R&D GTDS was used for orbit/attitude estimation for comparison with the sequential estimation by NAVPAK.

A number of numerical and force model options exist in the R&D GTDS. The spacecraft force model may be specified from simple two-body gravitational

force to a  $21 \times 21$  geopotential expansion. In addition, several atmosphere models are available as well as lunar/solar third body gravitational forces and solar radiation pressure. The integration of the spacecraft differential equations of motion may be done by Runge-Kutta methods (up to 8th order) or Cowell methods (up to 12th order). Spacecraft orbit propagation may also be done by variation-of-parameters methods or general perturbations techniques such as the Brower-Lyddane method.

The observation model used in the R&D GTDS for Landsat data is identical to that used in NAVPAK, including the attitude model. In Section 4, comparisons are made between batch estimation using the R&D GTDS and sequential estimation using NAVPAK.

## SECTION 3 - MATHEMATICAL MODELS

The observation and attitude models used in the R&D GTDS and Landsat NAVPAK systems are identical. As previously indicated, differences exist in the force model and numerical techniques used by each system for spacecraft orbit propagation. Also, the two systems use different estimation techniques. Both the estimation techniques and the spacecraft orbit propagation and numerical methods have all appeared in the literature. Hence, the detailed mathematics will not be presented here. On the other hand, the observation model and attitude models have not appeared in the literature. Thus, this section presents the Landsat observation model and attitude model.

### 3.1 OBSERVATION MODEL

The observation model in the R&D GTDS and Landsat NAVPAK is used to predict the observed picture coordinates (viz. the integer pair which specifies a location within the picture) as a function of an observation time  $t_s$ , a given satellite state vector  $(\bar{r}_o, \dot{\bar{r}}_o)$  at some epoch time,  $t_o$ , the satellite attitude time polynomial coefficients ( $R_o, R_1, \dots, R_4$  for roll,  $Y_i$  for yaw and  $P_i$  for pitch), camera biases  $(\alpha, \beta, \gamma)$  and the geodetic coordinates  $(\phi, \lambda)$  of a point on Earth which corresponds to the location within the picture. Instead of the integer pair  $(\ell, e)$  to specify locations within a picture, NAVPAK and the R&D GTDS models use an equivalent set of direction angles  $(\psi, \epsilon)$ . The transformation between  $(\ell, e)$  and  $(\psi, \epsilon)$  is developed in References 4 and 9. Slight modifications were made to the transformation constants to reflect experience with actual Landsat imagery. The observation time can be obtained from the time associated with the picture (scene) center,  $t_{ct}$  and the picture coordinates  $(\ell, e)$  by the linear relation developed in Reference 4. The time system used in the NAVPAK and R&D GTDS processing of Landsat data is Universal Time Coordinated (UTC).

In order to predict the angles  $\psi$  and  $\epsilon$  at a given time  $t$ , four basic coordinate systems are required.

Three of systems are shown in Figure 3-1, these are:

- $(x, y, z)$ --The geocentric inertial Cartesian coordinate system in which all of the basic computations, such as the numerical integration of the spacecraft equation of motion, are performed. The origin is at the center of the Earth and the  $z$  axis is along the Earth's axis of rotation positive towards the north pole. The  $x$  axis points towards the vernal equinox while the  $y$  axis completes the right hand orthogonal system. The  $(x, y, z)$  system is fixed in inertial space. A discussion of geocentric inertial coordinate systems (there are several, all available in the R&D GTDS, such as true-of-data, mean-of-1950, etc.) can be found in Reference 8 or any standard celestial mechanics text such as Reference 10.
- $(x', y', z')$ --The geocentric non-inertial cartesian coordinate system in which geodetic landmark coordinates  $(\phi, \lambda)$  are measured. In this coordinate system the  $x'$  axis points towards the intersection between the Greenwich meridian and the Earth's equator. The  $z'$  axis lies along the Earth's axis of rotation and  $y'$  completes the right hand orthogonal set. This system rotates with the Earth (viz., it is fixed with respect to surface of the Earth).
- $(\hat{i}, \hat{j}, \hat{k})$ --This is the instantaneous roll, pitch and yaw coordinate system. The  $(\hat{i}, \hat{j}, \hat{k})$  system is a moving "orbital" reference frame defined such that,

$$\hat{i} = \bar{j} \times \bar{k}, \quad \bar{j} = \frac{\bar{r}_s \times \bar{v}_s}{|\bar{r}_s \times \bar{v}_s|}, \quad \bar{k} = \frac{\bar{r}_s}{|\bar{r}_s|} \quad (3-1)$$

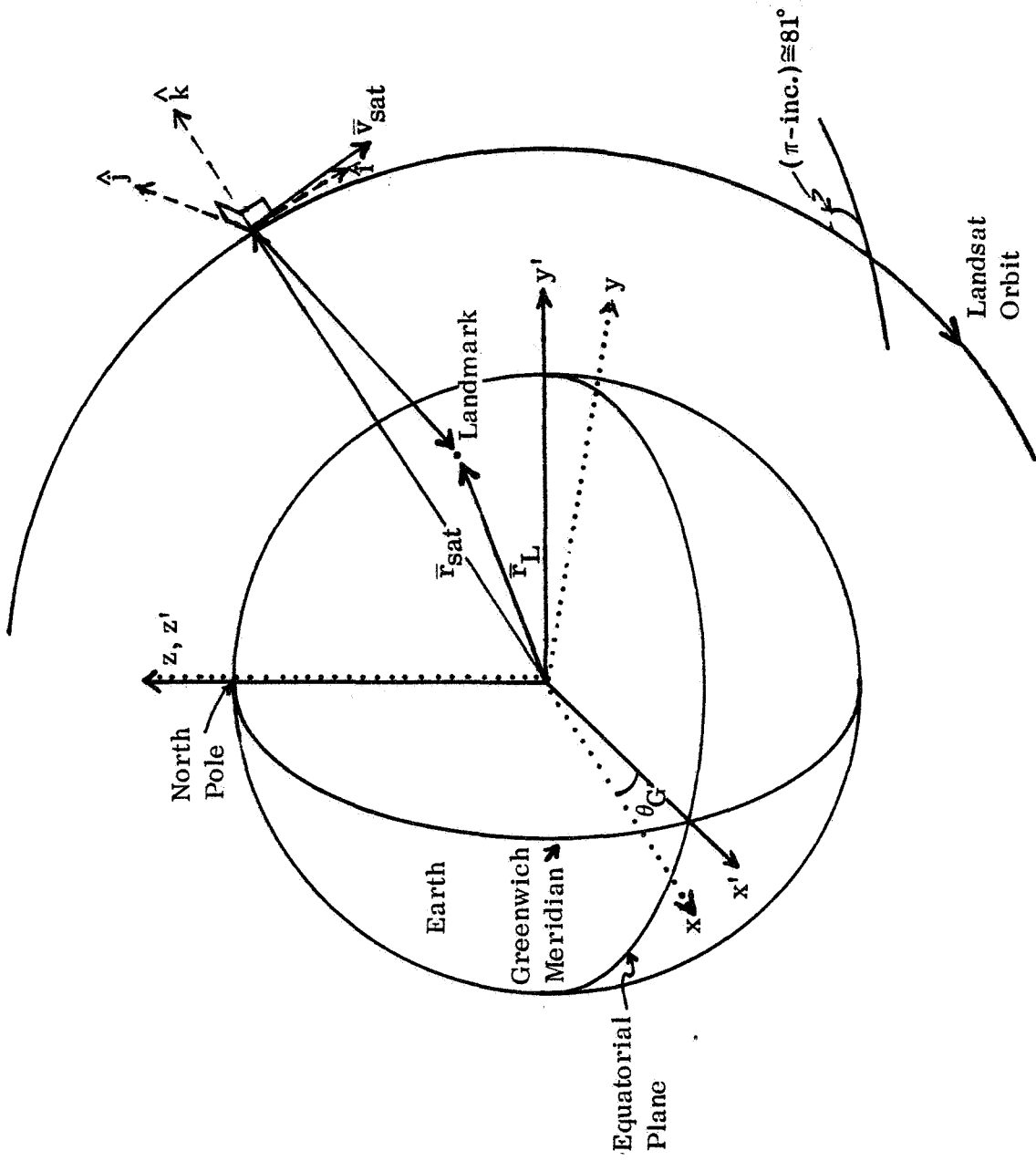


Figure 3-1. Landsat Orbit and Attitude Schematic

Note: A Landsat orbit and spacecraft nominal attitude are shown schematically relative to geocentric coordinates.

where  $\bar{r}_s$  and  $\bar{v}_s$  are the spacecraft position and velocity expressed in the (x, y, z) system. It is with respect to this system that the orientation of the spacecraft is measured.

The (x'', y'', z'') system represents the spacecraft body axis system. This coordinate system is centered at the spacecraft. The spacecraft is nominally aligned along the roll, pitch and yaw ( $\hat{i}$ ,  $\hat{j}$ ,  $\hat{k}$ ) frame. However, the time dependent misalignment between the spacecraft body system and the ( $\hat{i}$ ,  $\hat{j}$ ,  $\hat{k}$ ) frame is modeled by the attitude rotation matrix

$$S = \begin{pmatrix} \cos P \cos Y & \cos P \sin Y & -\sin P \\ -\cos R \sin Y + \sin R \sin P \cos Y & \cos R \cos Y + \sin R \sin P \sin Y & \sin R \cos P \\ \sin R \sin Y + \cos R \sin P \cos Y & -\sin R \cos Y + \cos R \sin P \sin Y & \cos R \cos P \end{pmatrix} \quad (3-2)$$

where R, P and Y are the time dependent roll, pitch and yaw angles discussed in Section 3.2.

Given the geodetic coordinates (geodetic latitude,  $\phi$ , and longitude,  $\lambda$ ) of a point on Earth the non-inertial geocentric cartesian coordinates (viz., the x', y', z') are found by the following transformation.

$$\bar{r}'_L = \begin{cases} s \cos \lambda \cos \varphi \\ s \sin \lambda \cos \varphi \\ s \sin \varphi (1 - E_e^2) \end{cases} \quad (3-3)$$

where the Earth's eccentricity,  $E_e$ , is

$$E_e^2 = 2 \cdot f - f^2 \quad (3-4)$$

where  $f$  is the flattening coefficient of the Earth ( $f \approx 1/298.3$ ), and  $s$  is the distance from the landmark to the  $z'$  axis measured along  $\vec{r}'_L$ . This is

$$s = \frac{R_e}{\sqrt{1 - E_e^2 \sin^2 \phi}} \quad (3-5)$$

with  $R_e$  the mean equatorial radius of the Earth. The Earth is represented as an ellipsoid, which has an  $x'$ ,  $y'$  plane circular cross section. Any plane which contains the  $z'$  axis intersects the ellipsoid to form an ellipse (meridian) of semimajor axis  $R_e$  and eccentricity  $E_e$ .

In order to represent  $\vec{r}'_L$  in the geocentric inertial coordinate system  $(x, y, z)$  the following transformation is performed

$$\vec{r}'_L = B(t)^{-1} \vec{r}'_L \quad (3-6)$$

where

$$B(t) = \begin{bmatrix} \cos [\theta_g(t)] & \sin [\theta_g(t)] & 0 \\ -\sin [\theta_g(t)] & \cos [\theta_g(t)] & 0 \\ 0 & 0 & 1 \end{bmatrix} \quad (3-7)$$

The angle  $\theta_g(t)$  is the time dependent Greenwich hour angle. The NAVPAK and R&D GTDS use the true-of-date system. NAVPAK evaluates  $\theta_g$  by Newcomb's expression which includes only precession effects, while the R&D GTDS evaluates  $\theta_g$  to include both precession and nutation. The use of the two different methods for determining  $\theta_g$  is of significance only when comparing the epoch S/C state vector components obtained by NAVPAK and R&D GTDS. The effect

on the observation residuals is negligible. In the R&D GTDS the evaluation of  $\theta_g(t)$  is made by accessing a data file created from a Jet Propulsion Laboratory (JPL) computer tape (see Reference 8).

The spacecraft position vector,  $\bar{r}_s$ , at the observation time,  $t$ , is determined from the estimated value of the spacecraft position vector,  $\bar{r}_{s_0}$  at an epoch time  $t_0$ . The method is to numerically integrate the second order differential equation of motion.

$$\frac{d^2 \bar{r}_s}{dt^2} = F(\bar{r}_s, \dot{\bar{r}}_s, t) \quad (3-8)$$

The R&D GTDS program has the options to perform this numerical integration by a variety of methods. The most accurate is a 12th order Cowell method. The Cowell method is discussed in Reference 11. The numerical integration of Equation (3-8) in NAVPAK is performed by a fourth-order Runge-Kutta method, using modified Fehlberg coefficients (Reference 12).

The total force,  $\bar{F}$ , on the satellite is modeled in NAVPAK to include atmospheric drag using a modified Harris-Priester model, two-body gravitational attraction of the Earth and the  $J_2$  non-spherical gravitational effect. The R&D GTDS has options to include a (21x21) spherical harmonic geopotential model of the Earth's gravitation, lunar/solar third-body gravitational forces, atmospheric drag and solar radiation pressure. Having obtained  $\bar{r}_L$  and  $\bar{r}_s$ , the inertial line-of-sight direction cosines  $\bar{\lambda}(\lambda_x, \lambda_y, \lambda_z)$  from the spacecraft to the landmark are

$$\bar{\lambda} = \frac{\bar{r}_L - \bar{r}_s}{|\bar{r}_L - \bar{r}_s|} \quad (3-9)$$

This line-of-sight unit vector can be transformed into the yaw-pitch-roll  $(\hat{i}, \hat{j}, \hat{k})$  frame by the transformation

$$\bar{\lambda}_o = T \bar{\lambda} \quad (3-10)$$

where

$$T = \left\{ \begin{array}{ccc} j_{oy}k_{oz} - j_{oz}k_{oy} & j_{oz}k_{ox} - j_{ox}k_{oz} & j_{ox}k_{oy} - j_{oy}k_{ox} \\ \frac{y_s \dot{z}_s - z_s \dot{y}_s}{L} & \frac{z_s \dot{x}_s - x_s \dot{z}_s}{L} & \frac{x_s \dot{y}_s - y_s \dot{x}_s}{L} \\ \frac{x_s}{|r_s|} & \frac{y_s}{|r_s|} & \frac{z_s}{|r_s|} \end{array} \right\} \quad (3-11)$$

where  $|r_s| = \sqrt{x_s^2 + y_s^2 + z_s^2}$

$L$  = angular momentum magnitude ( $|\bar{r}_s \times \bar{v}_s|$ ).

The transformation matrix  $T$  is simply the components of the  $\hat{i}, \hat{j}$  and  $\hat{k}$  given in Equation (3-1).

The line-of-sight unit vector may be expressed in the spacecraft body frame  $(x'', y'', z'')$  coordinate system by the rotation

$$\bar{\lambda}'' = S \bar{\lambda}_o = ST \bar{\lambda} \quad (3-12)$$

The  $S$  matrix is the attitude rotation matrix given by Equation (3-2). The modeling of these angles as a function of time is discussed in Section 3.2 of this paper. The  $S$  matrix is the result of a yaw, pitch and roll sequence of rotations.

Finally, the selected observables,  $\epsilon$  and  $\psi$ , must be related to the space-craft body frame line-of-sight direction cosines,  $\bar{\ell}''$ . It can be seen that

$$\epsilon = \arctan \left( \frac{\ell''_y}{\ell''_z} \right) \quad (3-13)$$

$$\psi = \arcsin \left( \frac{\ell''_x}{\ell''_y} \right)$$

provided  $\epsilon$  is an azimuthal angle measured (in the  $y'' z''$  plane) from the  $z'$ -axis, and  $\psi$  is an elevation angle from the  $z'' y''$  plane measured toward the  $x''$ -axis. Figure 3-2 shows these angles. (The reference axes of Reference 9 are related to those of Figure 3-2 by  $x' \rightarrow x''$ ,  $y'' \rightarrow y''$ ,  $z'' \rightarrow -z''$ ).

Equations (3-9), (3-12), and (3-13) represent the landmark observation model for any Earth-stabilized spacecraft in the absence of camera misalignments. If a misalignment exists, it may be represented by distinguishing the camera frame direction cosines  $\bar{\ell}'''$  from the spacecraft frame direction cosines  $\bar{\ell}''$ , and relating them via a misalignment matrix corresponding to small rotations  $\alpha$ ,  $\beta$ ,  $\gamma$  about the  $x''$ ,  $y''$ ,  $z''$  axes, respectively

$$\begin{pmatrix} \ell'''_x \\ \ell'''_y \\ \ell'''_z \end{pmatrix} = \begin{pmatrix} 1 & \gamma & -\beta \\ -\gamma & 1 & \alpha \\ \beta & -\alpha & 1 \end{pmatrix} \begin{pmatrix} \ell''_x \\ \ell''_y \\ \ell''_z \end{pmatrix} \quad (3-14)$$

or

$$\bar{\ell}''' = M \bar{\ell}'' \quad (3-15)$$

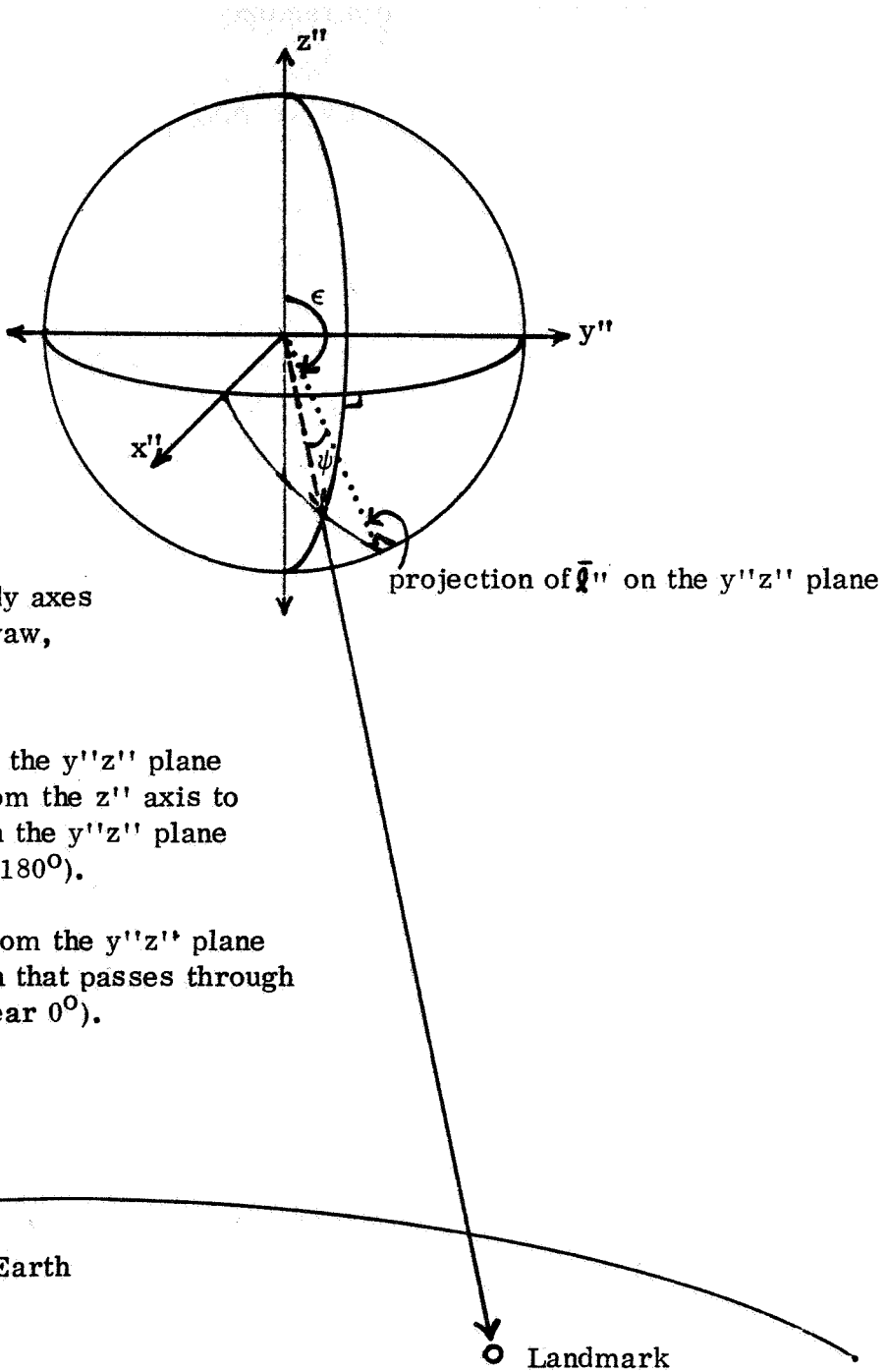


Figure 3-2. Observables for Landmark Model

where  $M$ , the misalignment matrix, is given by

$$M = \begin{pmatrix} 1 & \gamma & -\beta \\ -\gamma & 1 & \alpha \\ \beta & -\alpha & 1 \end{pmatrix} \quad (3-16)$$

The observation Equation (3-13) is then replaced with

$$\begin{aligned} \epsilon &= \arctan (\ell_y^m / \ell_z^m) \\ \psi &= \arcsin (\ell_x^m) \end{aligned} \quad (3-17)$$

### 3.2 ATTITUDE PROPAGATION MODEL

The Landsat satellite is a triaxially stabilized spacecraft in which momentum flywheels are used in a feedback system to attempt to stabilize the spacecraft's attitude against the variety of torques acting to change its attitude. Definitions of the roll, pitch, and yaw axes about which the spacecraft is stabilized are given in Section 3.1. The environmental torques causing inertial motion of the attitude (Y, P, R) frame are the aerodynamic torque caused by the Earth's atmosphere; the gravity-gradient torque due to the small difference in gravitational attraction from one end of the spacecraft to the other; the magnetic torque due to the interaction of the spacecraft's magnetic field with the Earth's magnetic field; and solar radiation and solar wind pressure acting on the spacecraft. In addition to these environmental torques, the spacecraft is influenced by internal activities (equipment functioning) and controls exerted by the spacecraft's attitude control system (ACS).

The process of determining the spacecraft attitude by modeling the attitude equations of motion while simultaneously determining the orbital parameters of the spacecraft is computationally difficult. For that reason, the current

attitude model used in the Landsat NAVPAK system and the R&D GTDS uses a simplified formulation that obviates the need for the complete integration of the attitude differential equations of motion.

The use of the monitored speed (rpm) of the stabilizing momentum wheels to aid in the attitude determination of the Landsat satellite was originally suggested by E. Lefferts and discussed in Reference 13. The wheel rate data from Landsat consists of forward and reverse wheel rates for roll and wheel rates for pitch and yaw in revolutions per minute given every second. The roll wheel rates are subtracted (forward-reverse) to obtain a net roll wheel rate. The use of wheel rate data to monitor the rapid attitude variations of Landsat is based on three assumptions:

- All disturbances that generate attitude motion for a three-axis stabilized spacecraft such as Landsat can be classified into the two following types: (1) environmental disturbance torques,  $N$ , or (2) errors and noise,  $\eta$ , in the sensors and the onboard ACS.
- The three channels (roll, pitch, and yaw) of the ACS are linear, continuous, and uncoupled, such that they can be treated independently.
- The attitude and wheel rate response due to the torques  $(a_N, \dot{a}_W)_N$  is independent of the response due to the noise  $(a_\eta, \dot{a}_w)_\eta$ .

Given these assumptions, the following equations are satisfied:

$$a(t) = a_N(t) + a_\eta(t) \quad (3-18)$$

$$\dot{a}_W(t) = \dot{a}_{W_N}(t) + \dot{a}_{W_\eta}(t) \quad (3-19)$$

where  $a$  is an attitude angle and  $\dot{a}_W$  is the reaction wheel rate.

The environmental disturbance torques,  $N$ , are near-deterministic and near-periodic at the orbital frequency and its low multiples. Examination of Landsat wheel rate data shows a large oscillation at the orbital period, which is believed to be due almost entirely to  $N$ . The torque contribution should also produce sizable components (particularly in roll and yaw) that are nearly constant over the orbital period. The disturbances arising from the noise,  $\eta$ , are largely random and should occur in a higher frequency regime than the main contributions from the environmental torques.

The attitude rates,  $\dot{a}_\eta$ , are related to the wheel rates,  $\dot{a}_{W_\eta}$ , as

$$\dot{a}_\eta = \frac{-I_W}{I} \dot{a}_{W_\eta} \quad (3-20)$$

where  $I_W$  is the moment of inertia of the reaction wheel and  $I$  is the moment of inertia of the spacecraft. This is valid because  $\eta$  produces, via the ACS, a wheel torque that drives both the reaction wheel and the spacecraft. The analogous equation for  $\dot{a}_N$  and  $\dot{a}_{W_N}$  is not correct, i.e.,

$$\dot{a}_N \neq \frac{-I_W}{I} \dot{a}_W \quad (3-21)$$

This is because the environmental torques,  $N$ , act directly on the spacecraft but not on the reaction wheel. Therefore, integration of the raw wheel rate

data will not produce an accurate attitude history. However, filtering the raw wheel rates to remove  $a_{W_N}$

$$\dot{a}_{W_\eta} = \dot{a}_W - \dot{a}_{W_N} \quad (3-22)$$

and integrating the  $\dot{a}_\eta$  derived from  $\dot{a}_{W_\eta}$  (note relationship between attitude rates and wheel rates in Equation (3-21)) should yield an accurate representation of  $a_\eta$ .

The attitude motion arising from the environmental torques,  $a_N$ , should be near-periodic in the mean orbital period,  $\bar{\omega}_0$ , such that

$$a_N \approx a_0 + a_1 t + a_2 \sin(\bar{\omega}_0 t + a_3) \quad (3-23)$$

Over a fractional period,  $a_N$  should be represented by a series expansion of the above equation:

$$a_N \approx a_0 + a_1 t + a_2 t^2 + a_3 t^3 + \dots \quad (3-24)$$

This representation of  $a_N$  is implemented in Landsat NAVPAK since data is processed only over a fraction of the orbital period. Both models (Equations 3-23 and 3-24) are implemented in the R&D GTDS.

The process of using wheel rate data for the representation of  $a_\eta$  requires that the low-frequency component of roll, pitch, and yaw wheel rate data be

removed. The low-frequency component is determined and removed by the following process:

1. The low frequency,  $\bar{\omega}_0$ , is input to a least squares program to fit the following trigonometric series to the raw wheel rate data:

$$\begin{aligned}\dot{a}_{W_N}(t) = & (A_1 + A_2 t) + (A_7 + A_8 t) \sin(\bar{\omega}_0 t) + (A_{13} + A_{14} t) \cos(\bar{\omega}_0 t) \\ & + (A_{19} + A_{20} t) \sin^2(\bar{\omega}_0 t) + (A_{24} + A_{25} t) \sin(\bar{\omega}_0 t) \cos(\bar{\omega}_0 t) \quad (3-25) \\ & + (A_{29} + A_{30} t) \sin^3(\bar{\omega}_0 t) + (A_{33} + A_{34} t) \sin^2(\bar{\omega}_0 t) \cos(\bar{\omega}_0 t)\end{aligned}$$

2. Using the coefficients ( $A_1$  through  $A_{34}$ ) obtained in Step 1, the Fourier series is evaluated at each wheel rate data point and subtracted to obtain a file of high-frequency wheel rate data.

$$\dot{a}_{W_\eta} = \dot{a}_W - \dot{a}_{W_N} \quad (3-26)$$

3. The high-frequency integrated wheel rates are then converted to body rates as follows:

$$\dot{a}_\eta = \frac{-I_W}{I} a_{W_\eta} \quad (3-27)$$

where  $I_W$  is the moment of inertia of the reaction wheel, and  $I$  is the moment of inertia of the spacecraft.

The low frequency,  $\bar{\omega}_0$ , contained in the wheel rate data is obtained through the maximum entropy method (MEM).

This MEM is a technique of performing a discrete Fourier analysis on data, subject to the constraint that the assumed ignorance (entropy) of data that are not given (data outside the given data interval) is a maximum. This is in contrast to the standard Fast Fourier Transform (FFT) in which implicit assumptions are made regarding data outside the given data span. The theory of the MEM is discussed in Reference 14 and the software used to perform in the spectral analysis is discussed in 15. Numerical experiments have shown that the MEM is superior to the FFT in its ability to extract low-frequency information from a given data set.

After a body rates file ( $\dot{a}_\eta(t)$ ) has been created by the process described above, then the attitude model is specified by Equation (3-18) where  $a_N(t)$  is approximated by Equation (3-24) and  $a_\eta(t)$  is obtained from  $\dot{a}_\eta(t)$  by a trapezoidal numerical integration. The coefficients of Equation (3-24) are either pre-specified or estimated in the orbit/attitude determination process.

## SECTION 4 - NUMERICAL RESULTS

Several numerical experiments have been performed with the Landsat NAVPAK and R&D GTDS using real landmark data. Prior to these experiments both software systems had been tested using simulated data. The numerical results must be considered as preliminary because of the limited data which was available. The data was generated using a single pass of Landsat-2 over the United States on April 15, 1977. There were 11 pictures available from New York to Florida. Landmark observations were created by the method discussed previously. The landmarks were selected at random throughout each picture with an attempt to cover the entire picture. United States Geological Survey maps (7-1/2 minute quadrangle size) were used to determine the geodetic coordinates of the landmarks. The data span and density were as follows: the first seven pictures of the pass (Time span 2 minutes, 50 seconds) contained 95 landmarks. The next two pictures were water scenes with no observable features providing a natural data gap of 1 minute and 12 seconds. The final two pictures contained 11 landmarks. The total data included 106 landmarks over a 4 minute, 46 second time span. For the same period wheel-rate data (R, P, Y) was available every second. The wheel-rate data was processed to obtain a high frequency body rate file by the previously indicated method.

### 4.1 R&D GTDS (BATCH DC) RESULTS

Several tests were made with the R&D GTDS using the landmark data. These tests included the effect of the choice of solve-for parameters, a priori covariance matrix, force model effects, and the use of wheel-rate data for attitude modeling. The results for each of these is discussed in this section.

#### 4.1.1 Choice of Solve-For Parameters

The available solve-for parameters in the R&D GTDS landmark model include six spacecraft state vector components (either geocentric inertial Cartesian or classical orbital elements), the five coefficients for each attitude (R, P, Y)

time polynomial, and three camera biases ( $\alpha$ ,  $\beta$ ,  $\gamma$ ). Other possible solve-for parameters such as drag coefficient, harmonic coefficients in the Earth's geo-potential model etc. are available. Only the first set of parameters (spacecraft state, attitude and camera biases) were used with the landmark data set. The data span is short enough so the other solve-for parameters cannot be realistically estimated.

It is well known that the addition of a solve-for parameter to a set of parameters to be estimated will decrease the residuals for a given data set. Thus, for example, estimating four parameters for a particular data set will result in smaller residuals than when only three of the parameters are estimated. This assumes that the parameters are observable (i.e., related to the observed quantities) and uncorrelated. Hence, using the complete solve-for set (spacecraft state, 15 attitude coefficients and camera biases) should produce the smallest residuals for the given data span. However, some of the parameters estimated in this manner are not particularly meaningful because of unobservability or high correlation among the solve-for parameters. The section addresses the question of how the choice of solve-for parameters affects the fit of the observational data.

The results for the full data span are shown in Table 4-1, which gives the rms residuals for the converged differential correction (DC) as a function of solve-for parameter set. The units of the residuals are pixels. When a parameter is not solved for, its value is specified as that which is annotated on the Landsat image file. This annotation contains values for the spacecraft state and constant attitude values, that is the first coefficient. The remaining attitude coefficients and camera biases were nominally set to zero when not solved for. In addition, the choice of a priori covariance matrix affected the final residuals. The covariance used was that determined by experiments described later in this section.

Several things are apparent from examining Table 4-1. First, the smallest residuals are obtained solving for the spacecraft state and 3 attitude coefficients (3 each for R, P, and Y). Slightly larger residuals are obtained when the spacecraft state and 2 attitude coefficients are solved for. The use of more than 3 attitude coefficients does not yield significantly smaller residuals. Of the three camera biases ( $\alpha$ ,  $\beta$ ,  $\gamma$ ), only the first one is observable over the data span used. Solving for the second or third (or both) camera biases does not produce smaller residuals than when they are not solved for. It is interesting to note that solving for the first camera bias gives the same rms residuals as solving for constant attitude coefficients. Indeed, over a short time span the camera bias coordinate rotation has the same effect as the attitude frame orientation. Over longer time spans the effects would be distinguishable. Results in Table 4-1 also compare the effect of solving for spacecraft state parameters compared to solving for attitude parameters.

#### 4.1.2 A Priori Covariance Matrix

Numerical experiments in Reference 16 had suggested that the relative weighting between orbit and attitude parameters in the priori covariance weighting should produce large differences in the resulting observation residuals. For that reason, experiments were performed with the real landmark data in which the spacecraft state was solved for along with one coefficient each for roll, pitch and yaw. The relative weighting between spacecraft state parameters and the attitude parameters was varied widely. The results are listed in Table 4-2, which shows the observation residuals as a function of a priori covariance. The overall residuals changed by a factor of about 1.5 over the large change in a priori covariance. The covariances associated with run number 6 were used for all the remaining DC runs in this section including those in Table 4-1. Run 6 was chosen over run 2, even though run 2 yielded very slightly smaller residuals, because of the number of iterations required.

Table 4-1. Observation Residuals as a Function of Solve-for Parameters

Run No.	Solve-for Parameters	Observation Residuals (pixels)			No. of DC Iterations to Converge
		Scan ( $\epsilon$ )	Elevation ( $\psi$ )	Total (rss)	
1	Spacecraft state only	14.0	10.2	17.3	7
2	State + $\alpha$	12.3	9.4	15.5	10
3	State + $\beta$	14.1	10.2	17.4	7
4	State + $\gamma$	14.0	10.2	17.3	7
5	State + $\alpha, \beta$	12.3	9.4	15.5	9
6	State + $\alpha, \beta, \gamma$	12.3	9.4	15.5	10
7	State + $\beta, \gamma$	14.1	10.2	17.4	7
8	State + $\alpha, \gamma$	12.3	9.4	15.5	9
9	State + 1 attitude coefficient	12.3	9.4	15.5	10
10	1 attitude coefficient only	16.9	12.1	20.8	3
11	State + 2 attitude coefficients	11.2	9.6	14.8	15
12	2 attitude coefficients only	17.6	12.3	21.5	3
13	State + 3 attitude coefficients	7.3	9.2	11.7	8
14	3 attitude coefficients only	11.0	11.9	16.2	3

**Solve-for Parameters:** Spacecraft state refers to six components ( $x, y, z, \dot{x}, \dot{y}, \dot{z}$ ) of the spacecraft geocentric inertial state vector; ( $\alpha, \beta, \gamma$ ) are the camera misorientation biases; attitude coefficients are the coefficients of the time polynomial for roll, pitch, and yaw (i.e., two attitude coefficients means the first two coefficients for roll, pitch, and yaw for a total of six attitude parameters).

**Observation Residuals:** Units are pixels.

**A Priori Covariances:**

$$\begin{aligned} \sigma_x^2 &= \sigma_y^2 = \sigma_z^2 = 25 \text{ km}^2 \\ \sigma_{\dot{x}}^2 &= \sigma_{\dot{y}}^2 = \sigma_{\dot{z}}^2 = .0025 \text{ km}^2/\text{sec}^2 \\ \sigma_0^2 &= 1 \text{ degree}^2 \\ \sigma_1^2 &= 1 \times 10^{-6} (\text{deg.}/\text{sec})^2 \\ \sigma_2^2 &= 1 \times 10^{-12} (\text{deg.}/\text{sec})^4 \end{aligned} \quad \left. \begin{array}{l} \text{attitude} \\ \text{coefficients} \end{array} \right\}$$

Table 4-2. Observation Residuals as a Function of  
A Priori Covariance Matrix

Run No.	A Priori Covariance			Observation Residuals (pixels)		
	$\sigma_x^2$	$\sigma_z^2$	$\sigma_R^2$	Scan ( $\epsilon$ )	Elevation ( $\psi$ )	Total (rss)
1	1	1	1	21.8	10.2	24.1
2	25	$0.25 \times 10^{-4}$	1	12.3	9.4	15.5
3	25	$0.25 \times 10^{-2}$	1	12.3	9.4	15.5
4	0.25	$0.25 \times 10^{-6}$	1	13.9	10.2	17.2
5	$0.25 \times 10^{-2}$	$0.25 \times 10^{-8}$	1	16.9	12.1	20.8
6	$25 \times 10^2$	$0.25 \times 10^{-2}$	1	12.3	9.2	15.4
7	25	$0.25 \times 10^{-4}$	$1 \times 10^{-4}$	14.3	12.1	18.7
8	25	$0.24 \times 10^{-4}$	$1 \times 10^{-2}$	12.7	9.7	16.0

Notes:

Units are kilometers<sup>2</sup>, (kilometers<sup>2</sup>/second<sup>2</sup>), and degrees<sup>2</sup>.

Although Run No. 6 shows the smallest residuals, it required 14 iterations for the DC to converge. Run No. 2 shows comparable residuals but required only 10 iterations for convergence. Hence, Run No. 2 was selected as the a priori covariance for the remaining runs in this section.

Only a single component each for the position, velocity, and attitude covariance is shown. The position components  $\sigma_x$ ,  $\sigma_y$ ,  $\sigma_z$  are identical. Similarly for velocity and attitude.

#### 4.1.3 Force Model Evaluation

The force model used in the Landsat NAVPAK system consists of the two-body Earth-satellite gravitational attraction with the added effects of  $J_2$  non-spherical gravitational potential term and atmospheric drag. A question which can be easily answered via the R&D GTDS is whether this force model is adequate over typical data spans to be encountered (i.e., approximately 5 minutes). As previously indicated, the R&D GTDS has available force models including two-body Earth-satellite gravitational attraction, non-spherical Earth gravitational potential models including  $J_2$  up to a  $21 \times 21$  spherical harmonics, several atmospheric drag models, third body lunar/solar gravitational effects and solar radiation pressure.

Several R&D GTDS runs were made using various force model combinations with actual landmark data. The residuals were compared to observe the effect of different force models. In all these runs state and 1 attitude coefficient were solved-for using the complete data span and every landmark. The a priori covariance was the same as that of the runs given in Section 4.1.2. These runs show that the residuals are not significantly affected by the choice of force model. In fact, the rms residuals differed by less than 0.01 pixel regardless of force model. Thus, the force model used in Landsat NAVPAK is an adequate one.

#### 4.1.4 Wheel-Rate Residuals

A lot of theoretical and software development has resulted from the contention that high frequency momentum wheel-rate data will aid in attitude modeling for Landsat (Reference 13). To test the contention a few runs were made using several solve-for parameter combinations with the 5-minute data span. In all cases, data density has been maintained as every landmark and the a priori covariances were those used in Section 4.1.2. The results presented in Table 4-3 compare the residuals for different choices of solve-for parameters.

Table 4-3. Effect of Wheel-Rate Data

Solve-for Parameters	Residuals (No Wheel-Rate Data)			Residuals (With Wheel-Rate Data)		
	Scan ( $\epsilon$ )	Elevation ( $\psi$ )	Total (rss)	Scan ( $\epsilon$ )	Elevation ( $\psi$ )	Total (rss)
Spacecraft state only	14.0	10.2	17.3	4.1	4.8	6.3
State + 1 attitude coefficient	12.3	9.4	15.5	3.1	3.6	4.8
State + 2 attitude coefficients	11.4	10.2	15.3	3.1	3.6	4.8
1 attitude coefficient only	21.5	12.8	25.0	18.5	9.1	20.6
2 attitude coefficients only	17.6	12.3	21.5	9.9	8.6	13.1
State + 3 attitude coefficients	7.3	9.3	11.8	2.7	3.6	4.5

Observation residuals are given as a function of solve-for parameters for the R&D GTDS DC. Two cases are shown. The left-hand results are without the use of wheel-rate data, while the right-hand results include wheel rate data. The units are pixels, and the a priori covariance matrix is the same as for Table 4-1. The data span is 5 minutes.

In all cases the wheel rate data decreased the observation residuals. Solving for S/C state and three attitude coefficients resulted in a total rss error of 4.5 pixels compared to the value of 11.8 without wheel rate data.

In addition to the overall residual decrease, the use of wheel rate data tended to stabilize the solution. Without wheel rate data, significant differences were obtained in the solve-for parameters when the three-minute and five-minute data spans were used. Specifically, the difference in magnitude of the S/C position vector between the five and three minute converged values was 11.4 km. The velocity vector magnitude changed by 0.021 km/sec. With wheel rate data, the changes were 2.9 km in position magnitude and 0.001 km/sec for velocity magnitude. Also, using wheel rate data the magnitude of the residuals stayed nearly the same using either a three minute or five minute data span. The implication here is that the use of wheel rate data stabilizes the solution so that less of a local fit phenomena is observed.

#### 4.2 LANDSAT NAVPAK (SEQUENTIAL) RESULTS

A number of experiments were performed using the Landsat NAVPAK extended Kalman Filter (EKF) for orbit/attitude estimation with the landmark data set discussed previously. Three areas are addressed including the choice of solve-for parameters, the a priori covariance matrix and the use of wheel-rate data. Prior to presenting the numerical results it should be mentioned that the NAVPAK (EKF) was an untuned filter. There was no process noise applied in the filter and no decaying memory. Moreover all results presented are based on a single pass of the filter through the data set. It is expected that the implementation of all of these features (i.e., decaying memory, process noise and iterative filter) will enhance the preliminary results presented here.

The NAVPAK filter was tested using simulated data both with and without added noise. These simulated data experiments provided a useful preparation for the use of actual landmark data.

#### 4.2.1 Choice of Solve-For Parameters

The effect of the choice of solve-for parameters for the NAVPAK EKF was investigated by trying a combination of parameter sets. The results are listed in Table 4-4 which gives the observation residuals (rms in pixel units) for several different solve-for parameter sets. A priori values of the parameters were obtained from the Landsat annotated images and the a priori covariance was selected based on results in Section 4.2.2. Two data spans are presented in Table 4-4. The three-minute span contains the data from the beginning of the Landsat pass up to the data gap. The five-minute span contains the entire data set discussed previously including the data gap. Observation residuals, used to compute the rms values in Table 4-4, were produced by propagating the final (last observation) EKF state vector back to the beginning of the data set and calculating residuals without further state corrections.

The smallest residuals are obtained by solving for the spacecraft state vector and one attitude coefficient each for roll, pitch and yaw. It is interesting to note that the rms residuals for the 3-minute span are usually smaller than the 5-minute span. This suggests a local fit situation in which the estimated parameters minimize the residuals but are not close enough to the true parameter values to exhibit the real noise level in the data.

Second and higher order attitude coefficients produced larger residuals than the first coefficient. Experiments with simulated data suggested that the filter closed down the a priori attitude covariance too rapidly to allow realistic estimation of these coefficients. The use of process noise may resolve this problem. Camera biases were not solved for. Experiments with simulated data indicated that the camera biases and attitude coefficient could not simultaneously be estimated realistically. This is caused by the fact that for a single observation the camera misalignment has an identical effect as a change in the constant attitude coefficients. The result was that solving for camera biases yielded

Table 4-4. Observation Residuals as a Function of Solve-for Parameters for NAVPAK

Run No.	Data Span (minutes)	Solve-for Parameters	Observation Residuals (pixels)		
			Scan ( $\epsilon$ )	Elevation ( $\psi$ )	Total (rss)
1	5	Spacecraft state only	15.0	15.5	21.6
2	3	Spacecraft state only	7.9	15.2	17.1
3	5	State + 1 attitude coefficient	14.7	11.9	18.9
4	3	State + 1 attitude coefficient	7.2	10.1	12.4
5	5	1 attitude coefficient only	18.6	12.6	22.5
6	3	1 attitude coefficient only	19.4	12.9	23.3
7	5	2 attitude coefficients only	44.3	50.9	67.5
8	3	2 attitude coefficients only	44.3	50.9	67.5
9	5	State + 2 attitude coefficients	100.5	119.4	156.1
10	3	State + 2 attitude coefficients	10.4	14.2	17.6

Observation residuals are given as a function of the choice of solve-for parameters. Parameters not solved for are set to the Landsat picture annotation values. The residuals are computed using the final EKF state propagated through the data set. Two time spans are given: a 3-minute time span, which includes the data from the beginning of the pass to the data gap; and a 5-minute span, which includes the data gap and the data after the gap. The a priori covariance values are:  $\sigma_x^2 = 1.0 \times 10^2 \text{ km}^2$ ;  $\sigma_{\dot{x}}^2 = 1.0 \times 10^{-2} (\text{km}^2/\text{sec}^2)$ ; and  $\sigma_R^2 = 1.0 \times 10^{-5} \text{ deg}^2$ .

identical results to solving for constant attitude biases. Again, the use of process noise may help this situation.

#### 4.2.2 A Priori Covariance Effect

Table 4-5 shows the results of varying the a priori covariance matrix in the NAVPAK EKF. Observation residuals are given as a function of a priori covariance matrix for the case in which the spacecraft state and one attitude coefficient are solved for. The rms residuals change by about 20 percent with a wide variation in the absolute values of the a priori covariance as well as a large change in relative weighting between spacecraft orbital and attitude parameters. Run number 4 yielded the lowest residuals so these values for the a priori covariance were used in the rest of this section.

#### 4.2.3 Wheel Rate Data Effects

The effect of wheel rate data using the Landsat NAVPAK system was investigated by performing the same computer runs as presented in Section 4.2.1 with the addition of wheel rate data for attitude modeling. The results are presented in Table 4-6, which gives the rms residuals for one pass through the data solving for various parameter combinations. The a priori covariances are the same as in Section 4.2.1. Comparison between Table 4-4 (without wheel rate data) and Table 4-6 (with wheel rate data) suggests several results. First, for the three-minute data span the wheel rate data does not provide significantly smaller residuals. Indeed for the case of solving for state plus one attitude coefficients the residuals are actually larger with wheel rate data. However, the 5-minute span does result in significantly smaller residuals using wheel rate data. The effect of the wheel rate data is to stabilize the attitude modeling over a data gap. A look at the residuals as a function of observation number indicated that the filter does not diverge (i.e., the solution degrading with propagation across the data gap) as much using wheel rate data as when wheel rate data is not used. The use of wheel rate data

also seems to allow for the realistic estimation of the second attitude coefficients. Such was not the case without wheel rate data.

Table 4-5. Observation Residuals as a Function of  
A Priori Covariance for NAVPAK

Run No.	A Priori Covariance			Observation Residuals (pixels)		
	$\sigma_x^2$	$\sigma_{\dot{x}}^2$	$\sigma_r^2$	Scan ( $\epsilon$ )	Elevation ( $\psi$ )	Total (rss)
1	$1.0 \times 10^4$	$1.0 \times 10^{-2}$	$1.0 \times 10^{-3}$	9.3	10.5	14.0
2	$1.0 \times 10^4$	1.0	$1.0 \times 10^{-3}$	9.1	10.5	13.9
3	$1.0 \times 10^6$	$1.0 \times 10^2$	$1.0 \times 10^{-3}$	8.3	10.4	13.3
4	$1.0 \times 10^2$	$1.0 \times 10^{-2}$	$1.0 \times 10^{-5}$	7.2	10.1	12.4
5	$1.0 \times 10^2$	$1.0 \times 10^{-2}$	$1.0 \times 10^{-1}$	10.7	11.0	15.3

Observation residuals are given as a function of the a priori covariance. The units are  $\text{km}^2$ ,  $(\text{km}^2/\text{sec}^2)$ , and  $\text{degrees}^2$ . The residuals are computed using the final EKF state, solving for the spacecraft state, and a constant attitude. The data span is 3 minutes.

Table 4-6. Effect of Wheel-Rate Data for NAVPAK

Solve-for Parameters	Data Span (minutes)	Observation Residuals (pixels) [With Wheel-Rate Data]		
		Scan ( $\epsilon$ )	Elevation ( $\psi$ )	Total (rss)
Spacecraft state only	5	10.3	15.1	18.3
Spacecraft state only	3	10.9	15.3	18.8
State + 1 attitude coefficient	5	12.2	9.2	15.3
State + 1 attitude coefficient	3	10.6	9.4	14.2
1 attitude coefficient only	5	27.9	12.2	30.4
1 attitude coefficient only	3	24.4	10.6	26.6
2 attitude coefficients only	5	34.2	53.0	63.1
2 attitude coefficients only	3	34.2	53.0	63.1
State + 2 attitude coefficients	5	25.3	60.8	65.8
State + 2 attitude coefficients	3	12.5	9.5	15.7

The observation residuals are shown as a function of solve-for parameters for NAVPAK. The covariance matrix is the same as in Table 4-4.

## REFERENCES

1. Computer Sciences Corporation, CSC/TM-75/6146, Landmark Observation Model for Earth Stabilized Satellites, P. S. Desai and H. Siddalingaiah, September 1975
2. --, CSC/TM-75/6147, Autonomous Navigation for TIROS-N and NIMBUS-6, P. S. Desai and H. Siddalingaiah, December 1975
3. --, CSC/SD-75/6058, GTDS Landmark Data Modeling, J. Fein, P. S. Desai and S. Wei, September 1975
4. --, CSC/SD-76/6054, Enhancements to the GTDS R&D Landmark and Picture Earth-Edge Data Capabilities, J. Fein, P. S. Desai, H. E. Stull, and F. L. Markley, September 1976
5. --, CSC/TM-77/6012, NAVPAK Design for Landsat and Kalman Filter Applications, E. M. O'Neill and H. E. Stull, January 1977
6. Goddard Doc. #76SDS4258 Landsat Data Users Handbook, September 2, 1976
7. Computer Sciences Corporation, CSC/SD-78/6173, Landsat NAVPAK System Description and User's Guide, S. R. Waligora, December 1978
8. National Aeronautics and Space Administration, Goddard Space Flight Center, S-582-76-77, Mathematical Theory of the Goddard Trajectory Determination System, edited by J. O. Cappellari, C. E. Velez, and A. J. Fuchs, April 1976
9. R. H. Caron and K. W. Simon, "Attitude Time-Series Estimator for Rectification of Spaceborne Imagery", Journal of Spacecraft and Rockets, vol. 12, #1, pp. 27-32
10. P. R. Escobal, Methods of Orbit Determination, 1965, John Wiley & Sons, Inc., New York
11. P. Henrici, Discrete Variable Methods in Ordinary Differential Equations, 1962, John Wiley & Sons, New York
12. D. G. Hull and D. G. Bettis, "Optimal Runge-Kutta Methods" (paper AA 575-080, presented at the AAS/AIAA Astrodynamics Conference, Nassau, Bahamas, July 1975)

## REFERENCES

13. Computer Sciences Corporation, CSC/TM-77/6115, Evaluation of Wheel Rate Data for Landsat Attitude Modeling, J. Fein, April 1977
14. J. G. Ables, "Maximum Entropy Spectral Analysis", Astronomy and Astrophysics Supplement, vol. 15, 1974, pp. 383-389
15. Computer Sciences Corporation, CSC/TM-77/6297, Maximum Entropy Spectral Analysis, D. L. Hall, November 1977
16. --, CSC/TM-78/6108, Error Analysis Structures on Orbit/Attitude Determination Using Landsat-1 and -2 Landmark Data, N. V. Kumar and D. L. Hall, December 1978